Received: 26 March 2024 | Revised: 16 July 2024 | Accepted: 16 July 2024

DOI: 10.1002/mp.17335

RESEARCH ARTICLE

MEDICAL PHYSICS

Analysis of hydrogen peroxide production in pure water: Ultrahigh versus conventional dose-rate irradiation and mechanistic insights

Tengda Zhang[1,2] | **Christina Stengl**[3,4] | **Larissa Derksen**[5] | **Kristaps Palskis**[6,7] | **Konstantinos Koritsidis**[1,8] | **Klemens Zink**[5,9,10] | **Sebastian Adeberg**[9,10,11] | **Gerald Major**[12,13,14] | **David Weishaar**[5] | **Ulrike Theiß**[10,15] | **Jing Jin**[16,17] | **Maria Francesca Spadea**[18] | **Elpida Theodoridou**[1,8] | **Jürgen Hesser**[2,19] | **Kilian-Simon Baumann**[5,9,10] | **Joao Seco**[1,20]

[1]Division of Biomedical Physics in Radiation Oncology, German Cancer Research Center, Heidelberg, Germany

[2]MIISM, Medical Faculty Mannheim, Heidelberg University, Mannheim, Germany

[3]Division of Medical Physics in Radiation Oncology, German Cancer Research Center, Heidelberg, Germany

[4]Medical Faculty Heidelberg, Heidelberg University, Heidelberg, Germany

[5]University of Applied Sciences, Institute of Medical Physics and Radiation Protection, Giessen, Germany

[6]CERN, Geneva, Switzerland

[7]Riga Technical University, Riga, Latvia

[8]Faculty of Physics, The Aristotle University of Thessaloniki, Thessaloniki, Greece

[9]Department of Radiotherapy and Radiation Oncology, Marburg University Hospital, Marburg, Germany

[10]Marburg Ion-Beam Therapy Center (MIT), Marburg, Germany

[11]Universitäres Centrum für Tumorerkrankungen (UCT) Frankfurt - Marburg, Marburg, Germany

[12]Department of Radiation Oncology, Heidelberg University Hospital, Heidelberg, Germany

[13]Heidelberg Institute of Radiation Oncology (HIRO), Heidelberg, Germany

[14]National Center for Tumor Diseases (NCT), Heidelberg, Germany

[15]Department of Radiotherapy and Radiation Oncology, Philipps-University, Marburg, Germany

[16]State Key Laboratory of Molecular Oncology and Department of Radiation Oncology, National Cancer Center/National Clinical Research Center for Cancer/Cancer Hospital, Chinese Academy of Medical Sciences (CAMS) and Peking Union Medical College (PUMC), Beijing, China

[17]Department of Radiation Oncology, National Cancer Center/National Clinical Research Center for Cancer/Cancer Hospital & Shenzhen Hospital, CAMS and PUMC, Shenzhen, China

[18]Institute of Biomedical Engineering, Karlsruhe Institute of Technology (KIT), Karlsruhe, Germany

[19]Interdisciplinary Center for Scientific Computing (IWR), Central Institute for Computer Engineering (ZITI), CZS Heidelberg Center for Model-Based AI, Heidelberg University, Heidelberg, Germany

[20]Department of Physics and Astronomy, Heidelberg University, Heidelberg, Germany

Correspondence
Kilian-Simon Baumann, University of Applied Sciences, Institute of Medical Physics and Radiation Protection, Giessen, Germany.
Email: kilian-simon.baumann@staff.uni-marburg.de

Abstract

Background: Ultrahigh dose-rate radiation (UHDR) produces less hydrogen peroxide (H_2O_2) in pure water, as suggested by some experimental studies, and is used as an argument for the validity of the theory that FLASH spares the

Joao Seco, Division of Biomedical Physics in Radiation Oncology, German Cancer Research Center, Heidelberg, Germany.
Email: j.seco@dkfz-heidelberg.de

Tengda Zhang, Christina Stengl, and Larissa Derksen are Co-shared first authors.
Killian-Siman Baumann and Joao Seco are Co-shared senior authors.

Funding information
Federal Ministry of Education and Research, Grant/Award Number: 02NUK076A; Hessen State Ministry of Higher Education, Research, and the Arts (HMWK), Grant/Award Numbers: LOEWE/2/16/519/03/09.001(0001)/101, 13FH726IX6; Deutsche Krebshilfe (DKH), Grant/Award Numbers: 70115332, 70115445

normal tissue due to less reactive oxygen species (ROS) production. In contrast, most Monte Carlo simulation studies suggest the opposite.

Purpose: We aim to unveil the effect of UHDR on H_2O_2 production in pure water and its underlying mechanism, to serve as a benchmark for Monte Carlo simulation. We hypothesized that the reaction of solvated electrons (e^-_{aq}) removing hydroxyl radicals (•OH), the precursor of H_2O_2, is the reason why UHDR leads to a lower G-value (molecules/100 eV) for H_2O_2 ($G[H_2O_2]$), because: 1, the third-order reaction between e^-_{aq} and •OH is more sensitive to increased instantaneous ROS concentration by UHDR than a two-order reaction of •OH self-reaction producing H_2O_2; 2, e^-_{aq} has two times higher diffusion coefficient and higher reaction rate constant than that of •OH, which means e^-_{aq} would dominate the competition for •OH and benefit more from the inter-track effect of UHDR. Meanwhile, we also experimentally verify the theory of long-lived radicals causing lower $G(H_2O_2)$ in conventional irradiation, which is mentioned in some simulation studies.

Methods and materials: H_2O_2 was measured by Amplex UltraRed assay. 430.1 MeV/u carbon ions (50 and 0.1 Gy/s), 9 MeV electrons (600 and 0.62 Gy/s), and 200 kV x-ray tube (10 and 0.1 Gy/s) were employed. For three kinds of water (real hypoxic: 1% O_2; hypoxic: 1% O_2 and 5% CO_2; and normoxic: 21% O_2), unbubbled and bubbled samples with N_2O, the scavenger of e^-_{aq}, were irradiated by carbon ions and electrons with conventional and UHDR at different absolute dose levels. Normoxic water dissolved with sodium nitrate ($NaNO_3$), another scavenger of e^-_{aq}, and bubbled with N_2O was irradiated by x-ray to verify the results of low-LET electron beam.

Results: UHDR leads to a lower $G(H_2O_2)$ than conventional irradiation. O_2 and CO_2 can both increase $G(H_2O_2)$. N_2O increases $G(H_2O_2)$ of both UHDR and conventional irradiation and eliminates the difference between them for carbon ions. However, N_2O decreases $G(H_2O_2)$ in electron conventional irradiation but increases $G(H_2O_2)$ in the case of UHDR, ending up with no dose-rate dependency of $G(H_2O_2)$. Three-spilled carbon UHDR does not have a lower $G(H_2O_2)$ than one-spilled UHDR. However, the electron beam shows a lower $G(H_2O_2)$ for three-spilled UHDR than for one-spilled UHDR. Normoxic water with N_2O or $NaNO_3$ can both eliminate the dose rate dependency of H_2O_2 production for x-ray.

Conclusions: UHDR has a lower $G(H_2O_2)$ than the conventional irradiation for both high LET carbon and low LET electron and x-ray beams. Both scavengers for e^-_{aq}, N_2O and $NaNO_3$, eliminate the dose-rate dependency of $G(H_2O_2)$, which suggests e^-_{aq} is the reason for decreased $G(H_2O_2)$ for UHDR. Three-spilled UHDR versus one-spilled UHDR indicates that the assumption of residual radicals reducing $G(H_2O_2)$ of conventional irradiation may only be valid for low LET electron beam.

KEYWORDS
hydrogen peroxide, solvated electron, ultrahigh dose rate, water radiolysis

1 | INTRODUCTION

Ultra-high dose rate (UHDR) irradiation used in FLASH radiotherapy, is a novel technique that delivers a high dose of radiation in a very short time to achieve a dose rate higher than 40 Gy/s. Several preclinical studies[1–3] have shown that FLASH radiotherapy can reduce normal tissue toxicity while maintaining tumor control, compared to conventional radiotherapy. This phenomenon, known as the FLASH effect, suggests that FLASH radiotherapy can widen the therapeutic window and has the potential to further increase the prescription dose against tumors that are radioresistant to conventional radiotherapy.

However, the radiobiological mechanisms underlying the FLASH effect are not yet fully understood. Ionizing radiation can cause direct deoxyribonucleic acid (DNA) damage but also ionize or excite water molecules in the human body, which is a physical process that generates various reactive oxygen species (ROS). These

TABLE 1 Reactions in water radiolysis and their reaction rate constants.[23,24,27]

Reaction no.	Reaction	Rate constant (10^{10} $M^{-1}s^{-1}$)	Reaction no.	Reaction	Rate constant (10^{10} $M^{-1}s^{-1}$)
1	$\bullet OH + H_2 \rightarrow H\bullet + H_2O$	0.0036	23	$H^+ + HO_2^- \rightarrow H_2O_2$	2
2	$\bullet OH + H_2O_2 \rightarrow HO_2\bullet + H_2O$	0.0033	24	$H_2O_2 \rightarrow H^+ + HO_2^-$	3.56×10^{-12}
3	$\bullet OH + O_2\bullet^- \rightarrow O_2 + OH^-$	0.9	25	$HO_2\bullet + H^+ \rightarrow O_2\bullet^-$	8×10^{-5}
4	$H\bullet + O_2 \rightarrow HO_2\bullet$	1.8	26	$H^+ + OH^- \rightarrow H_2O$	14.3
5	$H\bullet + O_2\bullet^- \rightarrow HO_2^-$	2	27	$H_2O \rightarrow H^+ + OH^-$	2.6×10^{-15}
6	$e_{aq}^- + O_2 \rightarrow O_2\cdot^-$	1.9	28	$H\bullet + \bullet OH \rightarrow H_2O$	2
7	$e_{aq}^- + H_2O_2 \rightarrow \cdot OH + OH^-$	1.2	29	$H\bullet + H\bullet \rightarrow H_2$	1
8	$e_{aq}^- + O_2\cdot^- \rightarrow HO_2^- + OH^-$	1.3	30	$\bullet OH + OH^- \rightarrow O\bullet^- + H_2O$	1.2
9	$e_{aq}^- + H^+ \rightarrow H\cdot$	2.2	31	$O\bullet^- + H_2O \rightarrow \bullet OH + OH^-$	0.00017
10	$e_{aq}^- + H_2O \rightarrow H\cdot + OH^-$	2×10^{-9}	32	$\bullet OH + O\bullet^- \rightarrow HO_2^-$	0.1
11	$e_{aq}^- + HO_2^- \rightarrow O\cdot^- + OH^-$	0.35	33	$\bullet OH + O_3\bullet^- \rightarrow O_2\bullet^- + HO_2\bullet$	0.85
12	$e_{aq}^- + H\cdot \rightarrow H_2 + OH^-$	2.5	34	$O\bullet^- + O_2 \rightarrow O_3\bullet^-$	0.3
13	$e_{aq}^- + e_{aq}^- \rightarrow H_2 + 2OH^-$	0.5	35	$O\bullet^- + H_2 \rightarrow H\bullet + OH^-$	0.008
14	$e_{aq}^- + \cdot OH \rightarrow OH^-$	3	36	$O\bullet^- + H_2O_2 \rightarrow H_2O + O_2\bullet^-$	0.02
15	$\bullet OH + \bullet OH \rightarrow H_2O_2$	0.55	37	$\bullet OH + HO_2^- \rightarrow HO_2\bullet + OH^-$	0.5
16	$\bullet OH + HO_2\bullet \rightarrow H_2O + O_2$	1.2	38	$HO_2^- + O\bullet^- \rightarrow OH^- + O_2\bullet^-$	0.08
17	$H\bullet + HO_2\bullet \rightarrow H_2O_2$	2	39	$O_3\bullet^- + H_2O_2 \rightarrow O_2\bullet^- + O_2 + H_2O$	0.00016
18	$H\bullet + H_2O_2 \rightarrow H_2O + \bullet OH$	0.009	40	$O_3\bullet^- + HO_2^- \rightarrow O_2\bullet^- + O_2 + OH^-$	8.9×10^{-5}
19	$H\cdot + OH^- \rightarrow e_{aq}^- + H_2O$	0.0021	41	$O_3\bullet^- \rightarrow O_2 + O\bullet^-$	3×10^{-8}
20	$HO_2\bullet + O_2\bullet^- \rightarrow O_2 + HO_2^-$	0.0089	42	$O_3\bullet^- + H_2 \rightarrow O_2 + H\bullet + OH^-$	2.5×10^{-5}
21	$HO_2\bullet + HO_2\bullet \rightarrow H_2O_2 + O_2$	0.0002	43	$O_2\bullet^- + H_2O_2 \rightarrow \bullet OH + O_2 + OH^-$	1.3×10^{-11}
22	$OH^- + H_2O_2 \rightarrow HO_2^- + H_2O$	0.0471	44	$HO_2\bullet + H_2O_2 \rightarrow \bullet OH + O_2$	5×10^{-11}

ROS react with each other because of free radical chain reactions, and they undergo diffuse transport simultaneously (shown in Table 1). This process, which lasts for about one microsecond, is called the inhomogeneous chemical reaction stage.[4] After that, the ROS distribution becomes relatively homogeneous, and the chemical reactions continue. This period of time is called the homogeneous chemical stage. ROS damages various molecules in the cell, including DNA, and triggers the subsequent biological response process. Since 60% of the human body is composed of water,[4] and since this radio-protective effect of UHDR has been observed in bacteria[5,6] as well, radiochemistry may play a significant role in the FLASH mechanism. Hydrogen peroxide (H_2O_2) is an important end product in the water radiolysis process and is also a major source of cellular oxidative stress and DNA damage due to the Fenton reaction.[7–10]

Previous studies have shown contradictory results regarding the dose-rate dependency of H_2O_2 production in pure water,[11–20] and most of Monte Carlo simulation studies have shown the opposite to recent experimental measurements. So far, there is no consensus on whether UHDR increases or decreases H_2O_2 yield compared with conventional irradiation. In addition, in previous research on H_2O_2 production, the hypoxic water samples did not contain carbon dioxide (CO_2) dissolved in the water. In contrast, there was 5% CO_2 in cell experiments to equilibrate the pH value of the medium. In addition to the dose-rate dependency, we also studied the role of CO_2 in the H_2O_2 yield.

Recent experimental[11,13,14,16] results suggest that UHDR has a lower G-value (molecules/100 eV) for H_2O_2 ($G[H_2O_2]$) without an explanation. We hypothesize that the mechanism behind this is that solvated electrons (e_{aq}^-) eliminate hydroxyl radicals (•OH), the precursor to H_2O_2, reducing $G(H_2O_2)$. In the case of UHDR, this scavenging of •OH becomes more effective since (Figure 1):

I. The reaction between the e_{aq}^- and •OH (reaction [14] shown in Table 1) has the highest reaction rate constant in the water radiolysis process except for the background reaction (26).

$$e_{aq}^- + \cdot OH \rightarrow OH^- \quad 3 \times 10^{10} M^{-1}s^{-1} \ (14)$$

The product of reaction (14) can also serve as the scavenger of •OH.

$$\bullet OH + OH^- \rightarrow O\bullet^- + H_2O \quad 1.2 \times 10^{10} M^{-1}s^{-1} \quad (30)$$

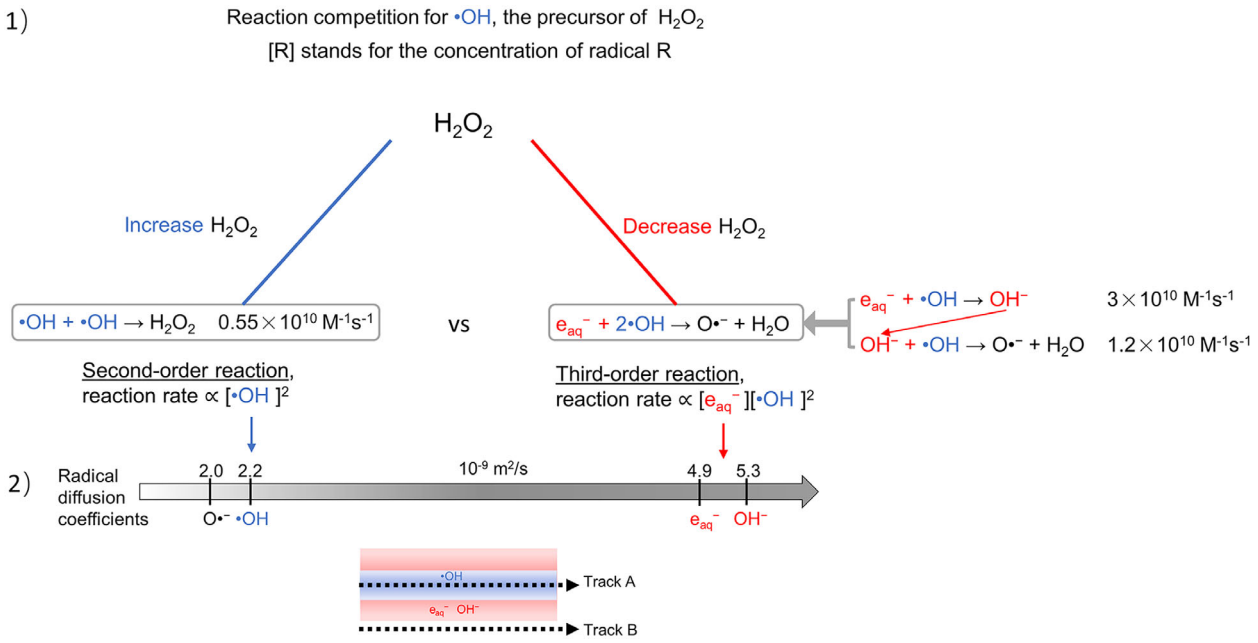

FIGURE 1 Two reasons why e_{aq}^- cause less H_2O_2 production in UHDR. (1), Third-order reaction is more sensitive to radical concentration change than second-order reaction, so the competition balance in conventional irradiation will shift toward the right side with UHDR increasing instantaneous radical concentration; (2), e_{aq}^- and OH– have higher diffusion coefficients and higher reaction rate constants than •OH, which means they would benefit more from the intertrack effect of UHDR, and remove •OH. H_2O_2, hydrogen peroxide; OH, hydroxyl radicals; UHDR, ultrahigh dose-rate radiation.

Therefore, we can combine reactions (14) and (30) into one reaction shown as the following:

$$e_{aq}^- + 2 \cdot OH \rightarrow O^{\cdot -} + H_2O \quad \text{extra (1)}$$

The main source of H_2O_2 is the recombination of •OH[12,21] which is the precursor to H_2O_2, as shown in the reaction (15).

$$\bullet OH + \bullet OH \rightarrow H_2O_2 \quad 0.55 \times 10^{10} M^{-1}s^{-1} \quad (15)$$

Evidently, there is a competition for •OH between reactions extra (1) and (15). Note that reaction (15) is a second-order reaction, while extra (1) is a third-order reaction. In conventional irradiation, these two reactions reach a competitive equilibrium. However, UHDR can increase the instantaneous radical concentration by several orders of magnitude in the same period of time, resulting in different enhancement of reaction rate because reaction extra (1), a third-order reaction, will benefit more from this concentration increase in the competition than reaction (15), a second-order reaction. The reaction rate for reaction extra (1) is $k_{extra(1)}[e_{aq}^-][\bullet OH]^2$ while the rate for reaction (15) is $k_{15}[\bullet OH]^2$, where $k_{extra(1)}$ and k_{15} stand for the reaction rate constant of each reaction and [radical] stands for the radical concentration. So, reaction extra (1) is more sensitive to concentration change than reaction (15). Hence, UHDR can shift the competition for •OH in conventional irradiation towards the reaction removing •OH, and lead to less H_2O_2 production.

II. Since both reactions (14) and (30) have higher reaction rate constants than •OH self-reaction and the primary yield[22,23] of e_{aq}^- is higher than the rest of radicals and molecules except for •OH and H^+, e_{aq}^- will dominate the competition for •OH. Also, the diffusion coefficients[24] of e_{aq}^-, OH^- and •OH are 4.9, 5.3, and 2.2×10^{-9} m^2/s, which means that e_{aq}^- will benefit more from inter-tract effect of UHDR[25] due to the higher diffusion rate.

To test the above hypothesis about e_{aq}^-, nitrous oxide (N_2O) gas, a solvate electron scavenger,[26] was used in our experiments. We expect to see that when e_{aq}^- is removed by N_2O, the H_2O_2 production has no difference in UHDR and conventional irradiation.

$$e_{aq}^- + N_2O \rightarrow N_2 + O^{\cdot -} \quad 0.91 \times 10^{10} M^{-1}s^{-1} \quad \text{extra(2)}$$

Most of the Monte Carlo simulations and analytical analysis[12,15,17,19,20] have shown that $G(H_2O_2)$ increases with increasing dose rate, which is the opposite of recent experimental results.[11,13,14,16] A model using molecular dynamics combined with Monte Carlo simulation suggests that UHDR produces less ROS, including H_2O_2, although it does not specifically show a decrease in only H_2O_2.[18] One assumption of higher $G(H_2O_2)$ by UHDR is that higher instantaneous •OH concentration increases the possibility of •OH recombination (reaction [15] in Table 1).[17] However, this assumption ignores that UHDR also increases the instantaneous concentration of e_{aq}^-, the scavenger of •OH, which has a higher reaction rate constant and

higher diffusion coefficient than •OH. Another explanation is that in conventional irradiation, the accumulation of relatively long-lived radicals in homogenous chemical stage, such as $O_2•^-$ and $HO_2•$, will affect the competition kinetics for the chemical species generated by the following pulses and remove H_2O_2 molecules,[12,15,19] as shown in reactions (43) and (44) in Table 1.

$$O_2 \cdot - + H_2O_2 \rightarrow \cdot OH + O_2 + OH^- \quad 1.3 \times 10^{-1} M^{-1} s^{-1} \quad (43)$$

$$HO_2 \cdot + H_2O_2 \rightarrow \cdot OH + O_2 \quad 5 \times 10^{-1} M^{-1} s^{-1} \quad (44)$$

To test this theory, we compared the H_2O_2 production of one-spilled UHDR and three-spilled UHDR. In three-spilled UHDR, each spill delivered the same dose as one-spilled UHDR, and there was at least a 5 s interval between each spill. In this way, the first UHDR spill would generate long-lifetime radicals that create the chemical environment described above to influence the chemical reactions of the radicals generated by the subsequent UHDR spills. So, we should observe that the $G(H_2O_2)$ of three-spilled UHDR is lower than that of one-spilled UHDR.

Previous studies[11,13,14,16] have used electron or proton UHDR to study H_2O_2 production. In our experiment, in addition to an electron beam, we used a carbon ion beam for the first time to study H_2O_2 production. Carbon ions and electron beams can deliver the same volume-averaged dose, but their microscopic dose distributions are entirely different because of the relatively high linear energy transfer (LET) of the carbon beam compared with the electron beam, which also results in different spatial distributions of ROS. This difference could have an impact on the chemical kinetics.

In conclusion, four main topics will be discussed in the following:

1. To test the theory of solvated electrons leading to low H_2O_2 production in UHDR with scavengers.
2. To define the impact of CO_2 on H_2O_2 production.
3. To test the long-lived radical theory by one-spilled UHDR versus three-spilled UHDR.
4. To determine the difference between high-LET carbon ions and low-linear energy transfer (low-LET) sources.

2 | MATERIALS AND METHODS

2.1 | Sample preparation

Water samples were prepared with varying oxygen concentrations by keeping Milli-Q water in a hypoxic chamber for at least 24 h:

1. hypoxic water with 1% O_2 and 5% CO_2,
2. real hypoxic water with 1% O_2 and 0.1% CO_2 (0% CO_2 is not allowed due to the hypoxic chamber setting limits),
3. and normoxic water with 21% O_2.

Therefore, three different water samples were used in the experiments. Different water samples were filled into 200 µL Eppendorf polymerase chain reaction (PCR) tubes, which are free of metal components (metal atoms would decompose H_2O_2 molecules), ensuring that there were no bubbles in the tubes. Pure N_2O gas (Guttroff, Germany) was used to bubble water at room temperature for 40 min in a gas-washing bottle to prepare the samples with N_2O. Sodium Nitrate ($NaNO_3$), another e^-_{aq} scavenger, was dissolved in normoxic water with the final concentrations of 25 and 250 µM and used in x-ray experiments. The pH values of water samples before and after dissolving N_2O and $NaNO_3$ were recorded using the Mettler Toledo pH Probe (Germany).

2.2 | Experimental setup and irradiation

2.2.1 | Carbon ion beam

A carbon ion beam was produced by synchrotron in the Marburg Ion-Beam Therapy Center. In our experiment, carbon ions were accelerated to 430.1 MeV/u, with a frequency of 6.74 MHz. 7.0×10^8 particles were injected into the synchrotron, which is the maximum number of particles that can be injected in one spill. The extraction time was 150 ms because after that, the extraction efficiency of the carbon ions decreased sharply (Figure 2a). Therefore, to achieve 40 Gy/s, at least 6 Gy was required within 150 ms. Even though the dose distribution in the sample is inhomogeneous, we expect the dose rate of each irradiated part of the sample to be higher than 40 Gy/s, so we do not need to worry about the ROS diffusion between the UHDR region and the non-UHDR region leading to any problem. The inner diameter of the 200 µL tube is approximately 5.5 mm. As shown in the dose profile in Figure 2b, the diameter of the region with a dose higher than 6 Gy is approximately 6 mm. Therefore, the samples were placed parallel to the beam direction with a 3D-printed sample holder (see Figure 2c) to ensure that the UHDR region covered the entire sample. An EBT-3 film was placed in front of each sample to record the received dose. One-spilled UHDR irradiation can deliver a volume-averaged dose of approximately 7 Gy, with a volume-averaged dose rate of approximately 50 Gy/s. Based on the dose measured from the one-spilled UHDR, conventional dose-rate irradiation (0.1 Gy/s) was adjusted to deliver a comparable dose. Three kinds of water samples with and without N_2O were irradiated under UHDR and conventional dose-rate conditions.

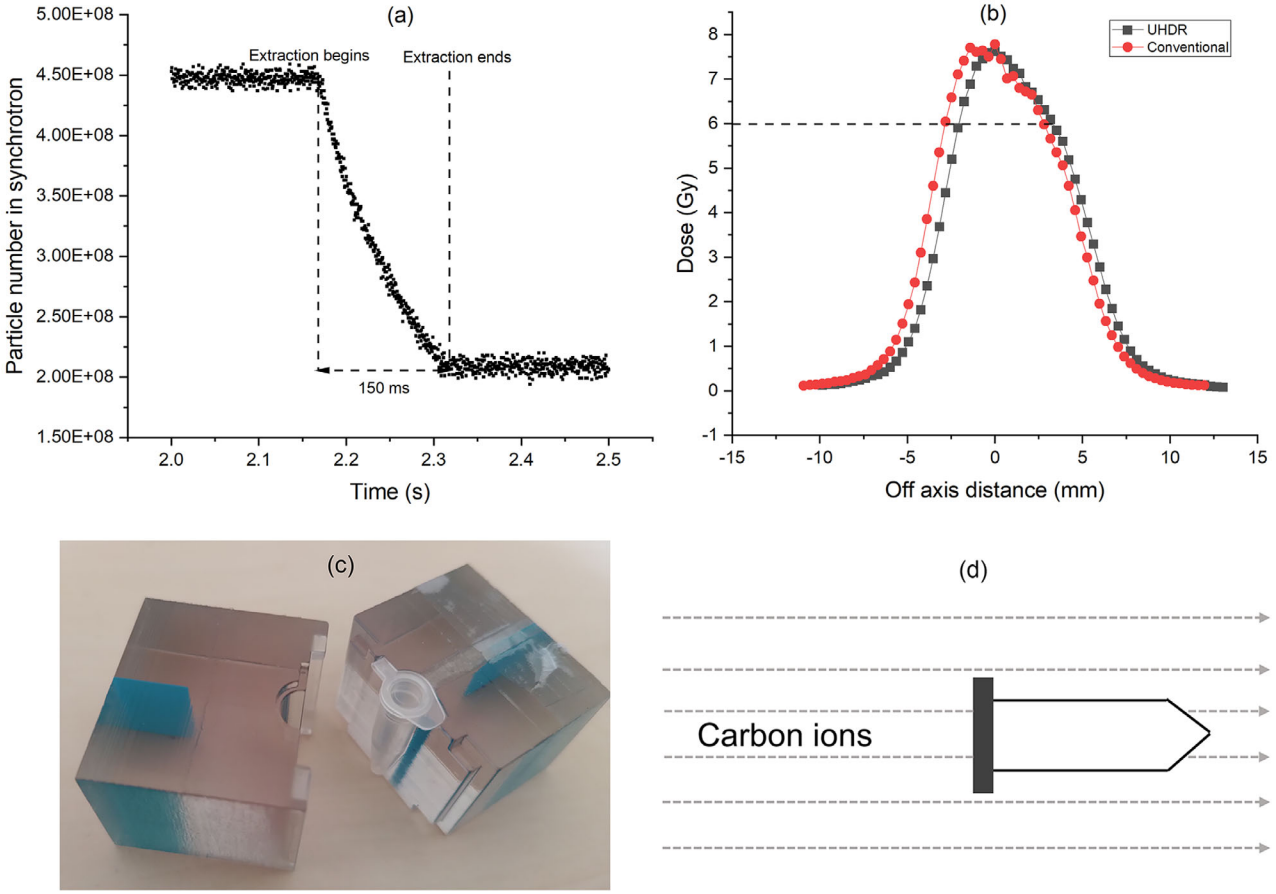

FIGURE 2 The irradiation setup used in carbon ion experiments. (a) The carbon ions extraction for UHDR lasting for 150 ms. (b) Exemplary dose profiles using carbon ions with UHDR and conventional dose rates. (c) The 3D-printed sample holder used to provide enough lateral scattering dose. (d) Sample tubes were placed horizontally. UHDR, ultrahigh dose-rate radiation.

For the comparison of the $G(H_2O_2)$ for one-spilled UHDR and three-spilled UHDR, the synchrotron requires at least 5 s of particle refilling time between two spills. We can assume that the first spill UHRD generates long-lifetime radicals that can affect the following chemical kinetics. In this experiment, only samples without N_2O were used.

2.2.2 | Electron beam

A 9 MeV electron source generated by a Mobetron unit (IntraOp Medical, Sunnyvale, CA, USA) with a field size of 6 cm was used in the experiment. The dose rate achieved for UHDR was 600 and 0.62 Gy/s for conventional irradiation. Dosimetry was performed using a FlashDiamond Detector T60025 (PTW, Freiburg, Germany). Mobetron can deliver a pulsed beam up to 3.6 μs pulse width with a pulse repetition frequency up to 120 Hz. Four-pulsed irradiation can achieve approximately 20 Gy within around 33.2 ms. To be consistent with the terminology of the carbon ion experiment, one-spilled UHDR consists of four pulses. The sample holder and experimental setup are shown in Figure 3. The irradiation schedule for the electron beam was the same as that for the carbon ions.

2.2.3 | x-Ray irradiation

As shown in Figure 4, MultiRad 225 (Precision, USA) irradiator was used to produce x-ray with dose rates of 0.1 and 10 Gy/s in the experiments, which is below the commonly recognized dose-rate threshold of 40 Gy/s for FLASH. The filter was removed to increase the dose rate. To further increase the dose rate, samples were placed close to the source by an elevatable rack. The voltage of the x-ray tube was set at 200 kV, and the current intensity was 17.8 mA. The irradiation dose for each sample is around 30 Gy.

2.3 | H_2O_2 measurement and statistics

CO_2 dissolves in water and forms carbonic acid, which lowers the pH of water. When the samples were saturated in a hypoxic chamber containing 5% CO_2, the pH decreased to around 6.4. Therefore, in the pH range of 6

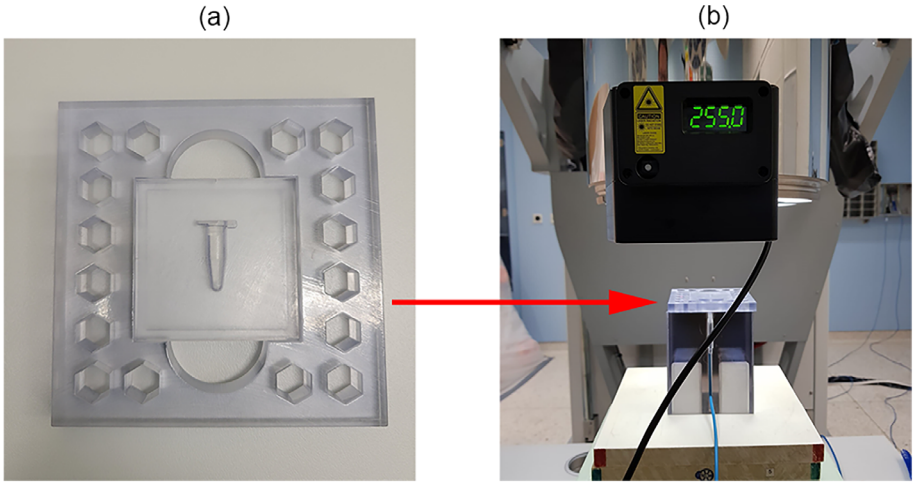

FIGURE 3 The experimental setup used in the 9 MeV electron irradiation. (a) The 3D-printed sample hold used in the experiments. (b) The electron facility, Mobetron, provides UHDR and conventional irradiation. UHDR, ultrahigh dose-rate radiation.

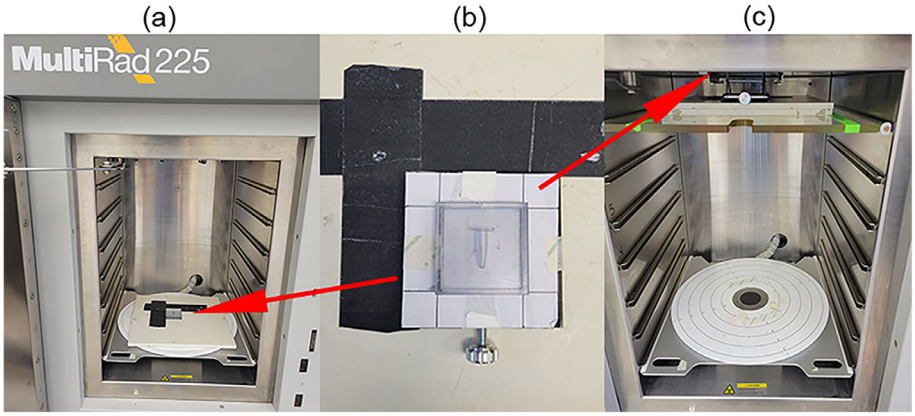

FIGURE 4 The experimental setup used in x-ray irradiation. (a) 0.1 Gy/s was achieved by positioning the samples on the lowest shelf. (b) The sample holder used in the experiment. (c) The samples were positioned on an elevatable rack to achieve around 10 Gy/s.

to 8, a pH-independent Amplex UltraRed assay (Thermo Fisher Scientific Inc, America), instead of the Amplex Red assay, was used to determine the concentration of H_2O_2 generated by irradiation. 50 μL of each irradiated sample was pipetted up and mixed with 50 μL of 100 μM Amplex UltraRed solution in a 96-well plate. The plate was covered with aluminum foil and incubated at room temperature for 40 min. Then, a plate reader was used to measure fluorescence intensity (excitation: 530 nm, emission: 590 nm). The system was fully calibrated by a series of fixed concentration of H_2O_2 solution. There were three samples for each oxygen condition, and the measurements of each sample were performed in triplicate. The Independent Samples *t*-test was used to assess the significance between the two groups. $P < 0.05$ was considered statistically significant.

3 | RESULTS

At extremely low pH values, the $G(H_2O_2)$ can dramatically increase. Therefore, the pH values of different water samples were monitored. Pure water has a pH of around 7. N_2O gas does not change the pH value. However, water samples dissolved 250 μM $NaNO_3$ and equilibrated at 5% CO_2, respectively, have pH values of 6.7 and 6.4.

3.1 | $G(H_2O_2)$ of the different kinds of water samples irradiated by carbon ions

As shown in Figure 5a, although hypoxic sample contains only 1% oxygen, similar to real hypoxic sample, it has the highest $G(H_2O_2)$ among three kinds of water because of the presence of 5% CO_2. Normoxic samples have a lower $G(H_2O_2)$ than hypoxic samples but higher than real hypoxic samples. It can be concluded that oxygen can increase the H_2O_2 production (real hypoxic vs. normoxic sample), and CO_2 can also markedly boost the H_2O_2 production (real hypoxic vs. hypoxic sample). Because the solubility of CO_2 is approximately 30 times higher than that of oxygen, hypoxic water equilibrated with 5% CO_2 has a higher H_2O_2 yield even than

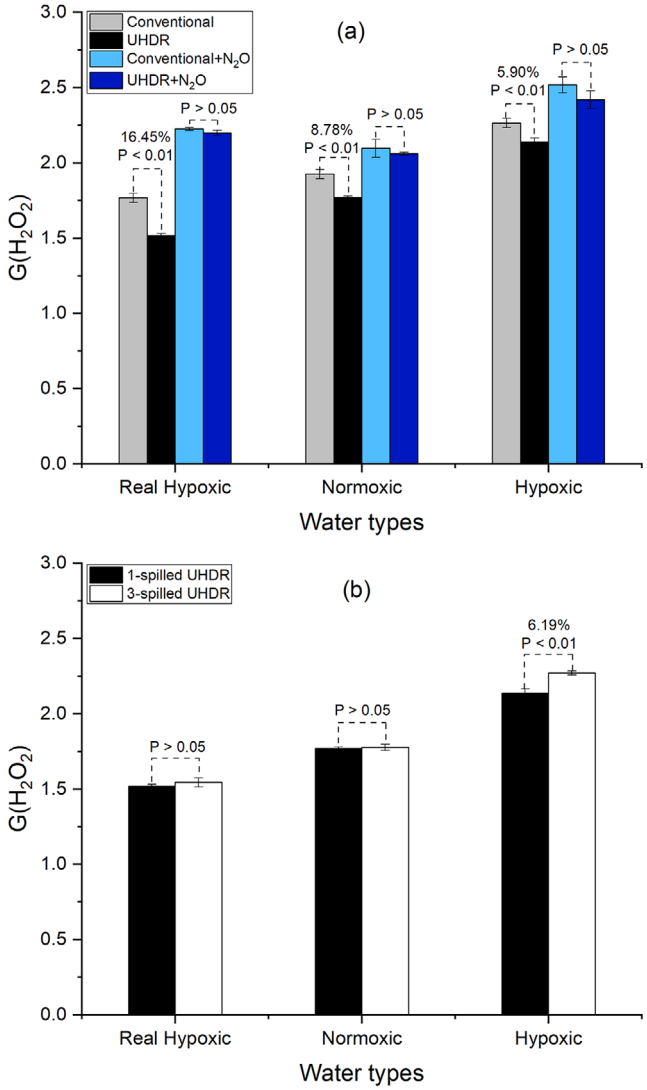

FIGURE 5 Radiolytic H_2O_2 yields of water samples with various O_2 and CO_2 concentrations irradiated by 430.1 MeV/u carbon ions. (a) The comparison of UHDR with conventional dose-rate irradiation for samples with and without N_2O. (b) $G(H_2O_2)$ of one-spilled UHDR and three-spilled UHDR. CO_2, carbon dioxide; H_2O_2, hydrogen peroxide; N_2O, nitrous oxide; OH, hydroxyl radicals; UHDR, ultrahigh dose-rate radiation.

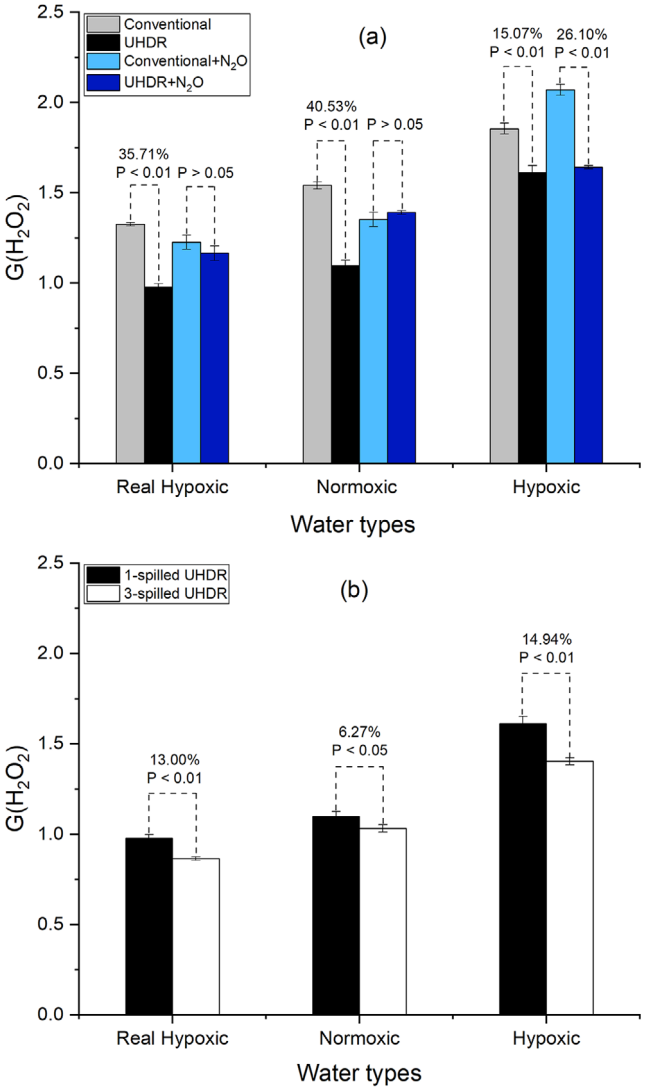

FIGURE 6 Radiolytic H_2O_2 yields of water samples with various O_2 and CO_2 concentrations irradiated by 9 MeV electron beam. (a) The comparison of UHDR with conventional dose-rate irradiation for samples with and without N_2O. (b) $G(H_2O_2)$ of one-spilled UHDR and three-spilled UHDR. CO_2, carbon dioxide; H_2O_2, hydrogen peroxide; N_2O, nitrous oxide; OH, hydroxyl radicals; UHDR, ultrahigh dose-rate radiation.

normoxic water samples with 21% oxygen (hypoxic vs. normoxic sample).

Furthermore, as we can see in Figure 5a, UHDR always produces less H_2O_2 than conventional irradiation for any type of sample without N_2O, which is similar to recent experimental results mentioned before. However, the difference between UHDR and conventional irradiation became statistically insignificant ($P > 0.05$) for all three kinds of samples with N_2O. Note that N_2O increases both $G(H_2O_2)$ of UHDR and conventional irradiation, while this effect is more pronounced for UHDR, resulting in eliminating the dose-rate dependency of H_2O_2 production.

In the end, as shown in Figure 5b, there is no significant difference in $G(H_2O_2)$ between one-spilled UHDR and one-spilled UHDR for both real hypoxic and normoxic water conditions, despite one-spilled UHDR appearing to produce slightly more H_2O_2. However, for hypoxic water with CO_2, one-spilled UHDR has a higher $G(H_2O_2)$ than one-spilled UHDR does.

3.2 | $G(H_2O_2)$ of various kinds of water samples irradiated by electron source

As shown in Figure 6a, like carbon ions, electron UHDR also has a lower $G(H_2O_2)$ than conventional irradiation,

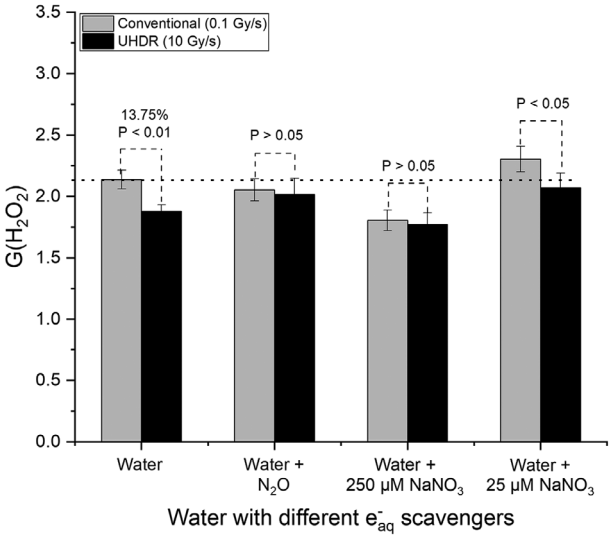

FIGURE 7 Radiolytic H_2O_2 yields of normoxic water samples with different e^-_{aq} scavengers, irradiated by 200 kV x-ray. $P < 0.05$ means statistically significant. H_2O_2, hydrogen peroxide.

but the difference between UHDR and conventional is even more significant. For real hypoxic water, the difference in $G(H_2O_2)$ can be up to around 35%, and for normoxic water, it can reach around 40%. For the three different water samples, we can still observe that $G(H_2O_2)_{hypoxic} > G(H_2O_2)_{normoxic} > G(H_2O_2)_{real\ hypoxic}$, which is consistent with the $G(H_2O_2)$ of carbon ions. For carbon ions, N_2O increases both UHDR and conventional $G(H_2O_2)$ while eliminating the discrepancy between them. However, we can see that N_2O has a different impact on H_2O_2 production with electron beams than with carbon ions. (1), for real hypoxic and normoxic samples, N_2O can also eliminate the difference in H_2O_2 yield between electron UHDR and electron conventional irradiation by decreasing the $G(H_2O_2)$ of conventional irradiation, which is opposite to carbon ions but increasing the $G(H_2O_2)$ of UHDR, resulting in the previous 35.71% and 40.53% difference between UHDR and conventional becoming statistically insignificant. (2), for hypoxic water with CO_2, on the contrary, N_2O increases the $G(H_2O_2)$ of conventional irradiation but does not have the same effect on the UHDR. The results of the comparison of G(H2O2) between one-spilled UHDR and three-spilled UHDR are shown in Figure 6b. Unlike carbon ion, the $G(H_2O_2)$ of three-spilled electron UHDR is always lower than that of one-spilled UHDR, and this effect is the same on three kinds of water samples.

3.3 | $G(H_2O_2)$ of water with different scavengers irradiated by kV x-ray

There is around 13.75% difference in $G(H_2O_2)$ of pure water between x-ray conventional and UHDR, as shown in Figure 7. N_2O can also eliminate the dose-rate dependency of $G(H_2O_2)$ in x-ray experiments, just like in carbon ion and electron beam experiments. However, compared to carbon ions, x-ray is also a low LET source, just like the electron beam, and its $G(H_2O_2)$ is similarly modified by N_2O as the previous electron beam, that is, N_2O only increases the $G(H_2O_2)$ of UHDR. Another e^-_{aq} scavenger, $NaNO_3$, can also eliminate or narrow the difference in H_2O_2 production between conventional and UHDR, resulting in no statistical significance ($P > 0.05$). Note that 250 μM $NaNO_3$ decreases $G(H_2O_2)$ of the conventional dose rate irradiation, but 25 μM $NaNO_3$ increases the G-value.

4 | DISCUSSION

About 60 years ago,[28–30] when researchers discovered that ultra-high dose rate mode could improve the survival fraction of cells after irradiation, radical-radical recombination was a popular hypothesis proposed in the early days.[31] Due to the higher instantaneous radical concentration produced by ultra-high dose rate irradiation, the probability of radical recombination increases, resulting in less ROS production, thereby improving the survival fraction of cells after irradiation. H_2O_2, as a relatively stable ROS, is an important end product of water radiolysis. Recent studies[11,13,14,16] have shown that compared with conventional irradiation, UHDR generates less H_2O_2 without providing an explanation. However, except for one study,[18] most Monte Carlo simulations and analytical analyses have shown the opposite.[12,15,17,19,20] Therefore, even with regard to the question of H_2O_2 production in UHDR, there is no consensus in the academic community. An assumption from studies claiming UHDR increases $G(H_2O_2)$ is that higher instantaneous •OH concentration favors •OH recombination (reaction [15] in Table 1), resulting in more H_2O_2.[17] Another assumption claiming UHDR produces more H_2O_2 attributes this to some long-lived radicals, such as $O_2•^-$ and $HO_2•$, accumulating in conventional irradiation and affecting the subsequent chemical reaction kinetics, resulting in conventional irradiation producing less H_2O_2 than UHDR.[12,15,19]

From our results, we can see that for the three water samples with different O_2 and CO_2 concentrations, whether using an electron beam with a uniform microscopic dose distribution or a carbon ion beam with a very heterogeneous microscopic dose distribution, UHDR always decreases $G(H_2O_2)$ compared to conventional irradiation. •OH is the precursor of H_2O_2, and previous studies[12,21] have indicated that reaction (15) in Table 1 is the primary source of H_2O_2 produced by water radiolysis. As we described before, e^-_{aq} is the main scavenger of •OH because of its high rate constant and primary yield, and we showed the effects of e^-_{aq} on removing •OH is the reason behind less H_2O_2 production of UHDR.

4.1 | Solvated electron scavengers removing the dose-rate dependency of H_2O_2 production

4.1.1 | Carbon ion source

To verify our theory about e^-_{aq} mentioned before, we introduced N_2O in the experiment. N_2O can react with e^-_{aq} and generate chemically stable N_2 and oxygen atomic anion ($O\bullet^-$). $O\bullet^-$ can react with many kinds of radicals, including •OH, but the reaction rate constant is only 0.1×10^{10} $M^{-1}s^{-1}$, as shown in reaction (32) in Table 1, which is lower than that of the reaction between e^-_{aq} and •OH (3×10^{10} $M^{-1}s^{-1}$), and even lower than that of the self-reaction of •OH producing H_2O_2 (0.55×10^{10} $M^{-1}s^{-1}$). In the experiment with carbon ion beam, eliminating e^-_{aq} by N_2O reduces the scavenging capacity for •OH, so we can see that the $G(H_2O_2)$ increase under both UHDR and conventional irradiation. Meanwhile, N_2O eliminates the third-order reaction extra (1), so the competition balance in conventional will not shift toward removing •OH when UHDR increases the instantaneous radical concentration; thus, there is no dose-rate dependency of $G(H_2O_2)$ for carbon-ion irradiation as shown in Figure 5a. Another experiment[32] conducted in 1968 also supports our e^-_{aq} theory. In that experiment, researchers found out dose-rate independence of $G(H_2O_2)$ when they irradiated $HClO_4$ water solution with a pH = 0.46. In an extreme acid environment, all e^-_{aq} can be eliminated by H^+ (reaction [9] in Table 1) with an even higher rate constant than N_2O.

4.1.2 | Electron source

For real hypoxic and normoxic water with the electron beam, although N_2O still eliminates the difference in H_2O_2 production between UHDR and conventional irradiation, similar to its effect in the carbon ion experiment, it decreases the $G(H_2O_2)$ of conventional irradiation (Figure 6a). We can see this phenomenon because of the relatively high concentration of N_2O compared to ROS concentration.[21] N_2O, as a scavenger of e^-_{aq}, can also react with e^-_{pre} (the precursor of e^-_{aq}) and molecular cation of water (H_2O^+) if the relative concentration is high enough. The dissociative recombination reaction of e^-_{pre} with H_2O^+ is one of two sources of •OH. Therefore, a relatively high concentration of N_2O leads to lower •OH production. That study has shown that with increasing concentration of scavenger of e^-_{aq}, $G(H_2O_2)$ increases at the beginning and then decreases at high scavenger concentration(Figure 7 in that paper).[21] In our experiment, we dissolved N_2O in water by bubbling the gas. It was hard to control the accurate scavenger concentration, so we chose to saturate N_2O to maintain the same experiment conditions each time. The reason why we see that N_2O still increases the $G(H_2O_2)$ of conventional irradiation of carbon ion beam is that the relatively high LET of carbon ions leads to the microscopic dose distribution being very heterogeneous. Although the volume-averaged dose is only a few Gy, the microscopic dose near the carbon ion tracks can exceed 1000 Gy,[33,34] so the local dose rate is significantly higher than 50 Gy/s used in carbon ion UHDR. Most of the ROS produced by carbon ions are distributed in the vicinity of carbon ion tracks, so the local ROS concentration is very high even under conventional irradiation, unlike the ROS produced by electron beam, which are uniformly distributed. This highly concentrated local ROS distribution makes N_2O concentration relatively low, resulting in the increased $G(H_2O_2)$ under conventional irradiation of carbon ion beam.

However, N_2O does not eliminate the dose-rate dependency of H_2O_2 production for hypoxic samples (1% O_2, 5% CO_2) with the electron source, as shown in Figure 6a. Apparently, this is because of the extra 5% CO_2. As for why we cannot see similar results using a carbon ion source, we believe it also relates to the relative concentration of CO_2 and N_2O compared to local ROS concentration. High local ROS concentration produced by high LET carbon ions minimizes the influence of CO_2 and N_2O. We will discuss the role of CO_2 in the following section.

In addition to e^-_{aq}, H• also serves as the scavenger for •OH with a relatively high reaction rate constant (2.5×10^{10} $M^{-1}s^{-1}$). The reason why we mainly focus on e^-_{aq} is that the primary yield of H• is only one-fifth of e^-_{aq}.[23] The "scavenging capacity" mentioned before is equal to the reaction rate constant × concentration,[15] so the concentration of the reactant is as important as the reaction rate constant in determining the scavenging capacity. Therefore, H• is not as important as e^-_{aq}, but we admit that H• also has an impact on H_2O_2 production.

4.1.3 | x-Ray source

As discussed above, the $G(H_2O_2)$ of the water sample with e^-_{aq} scavenger depends on the relative scavenger concentration. With x-Ray source, we could also see the similar results shown in Figure 7. x-Ray, like the electron beam, is classified as low-LET radiation, characterized by a uniform spatial dose distribution, resulting in low local ROS concentrations. In contrast, the relative concentration of N_2O is higher, so even though it scavenges e^-_{aq}, it does not increase $G(H_2O_2)$. However, due to the removal of e^-_{aq} by N_2O, the dose rate dependency of $G(H_2O_2)$ is also eliminated. In our x-ray experiments, we used another scavenger of e^-_{aq}, $NaNO_3$, which can also eliminate the dose rate dependency of $G(H_2O_2)$. We observed that 250 μM $NaNO_3$ not only eliminated the difference in H_2O_2 production between UHDR and conventional irradiation but also reduced the $G(H_2O_2)$ at conventional irradiation. Conversely, 25 μM $NaNO_3$

increased both UHDR and conventional $G(H_2O_2)$. However, because the concentration is not high enough, and its reaction rate constant with solvated electron is 0.97×10^{10} $M^{-1}s^{-1}$, its scavenging capacity is not high enough to eliminate the dose rate dependency.

The previous study,[21] along with our results in Figure 7 regarding different $NaNO_3$ concentrations, clearly demonstrate that the effect of the scavenger on $G(H_2O_2)$ depends on the relative concentration to ROS, which determines whether $G(H_2O_2)$ increases or decreases. Notably, $NaNO_3$ has a reaction rate constant with the precursor of e^-_{aq} that is at least an order of magnitude higher than that of N_2O,[21] but similar rate constant with e^-_{aq}, which means $NaNO_3$ tends to remove the precursor, compared to N_2O, easily leading to a lower $G(H_2O_2)$. Both compounds, serving as e^-_{aq} scavengers, eliminate the dose rate dependency of H_2O_2 production, strongly supporting our hypothesis.

4.2 | One-spilled UHDR versus three-spilled UHDR

Previous studies,[12,17,20] especially Monte Carlo simulations, suggested that UHDR should increase the $G(H_2O_2)$, and explained that some radicals, such as $O_2{\bullet}^-$and $HO_2{\bullet}$, would persist for a much longer time in conventional irradiation than other radicals and affect the chemical reaction kinetics of the free radicals produced by subsequent irradiation, thereby reducing the production of H_2O_2. This effect is insignificant for UHDR irradiation because UHDR delivers all dose in a very short time, so the $G(H_2O_2)$ of UHDR is higher than that of conventional irradiation. This theory seems reasonable to some extent, but it ignores the fact that the concentration of those residual long-lived radicals in the homogeneous chemical stage is very low, as shown in their own Monte Carlo studies. To verify this hypothesis, we designed an experiment of one-spilled UHDR versus three-spilled UHDR. In three-spilled UHDR irradiation, there is at least a 5 s interval between each spill, and the first spill produces many long-lived radicals that affect the chemical kinetics of the following two spills, just like conventional irradiation. If the hypothesis is true, we should see that the $G(H_2O_2)$ of three-spilled UHDR is lower than that of one-spilled UHDR. However, as shown in Figures 5b and 6b, the $G(H_2O_2)$ of three-spilled UHDR is lower than that of one-spilled UHDR in the experiment using electron beam, but we do not see the same situation with the carbon ions. One possible reason is the different spatial distribution of radicals produced by carbon ions and electrons. Although those long-lived radicals have been found to survive for hours after irradiation, their concentration becomes very low after 1 microsec of irradiation,[12,35] which is the start of the homogeneous chemical stage. The radicals produced by carbon ion beams are highly concentrated in the vicinity of the carbon ion tracks. The local concentration of the newly produced free radicals is several orders of magnitude higher than that of the previous residual free radicals, so the concentration of residual radicals is not high enough to affect the chemical kinetics of the radicals produced by subsequent carbon ion beams. The radical spatial distribution produced by the electron beam is homogeneous, and the local radical concentration is low. Therefore, residual radicals affecting subsequent chemical reactions only occur in low-LET beams like electron beams.

Another reason is that a high LET carbon ion beam can produce O_2 in tracks because of multiple ionization,[7,8] and another study also suggested that carbon ions can generate highly oxygenated conditions in the tumor environment.[36] O_2 can increase H_2O_2 production so that it can counteract those long-lived radicals.

As for the reason why three-spilled carbon ion UHDR has a higher $G(H_2O_2)$ than one-spilled carbon ion UHDR for hypoxic water (1% O_2 and 5 % CO_2), we will discuss the effect of CO_2 in the next section.

4.3 | The role of CO_2 in water radiolysis

Our experiment has shown that O_2 can increase H_2O_2 production. Studies on ROS production and radiosensitivity often only consider the role of O_2 and ignore CO_2. Because the role of CO_2 in the cell culture environment is often only assumed to maintain physiological pH levels. According to Henry's law constants,[37] the solubility of CO_2 is around 26 times that of O_2 under the same conditions, and metabolically active tissues consume more O_2 and produce more CO_2. If we want to study the role of ROS production in UHDR, CO_2 should not be ignored. Our experiments have shown that the hypoxic sample containing CO_2 has the highest $G(H_2O_2)$ among the three kinds of water samples, no matter for carbon ions or electron beam. As mentioned before, the pH value of water equilibrated with 5% CO_2 drops to around 6.4, and the acid chemical environment favors H•, which is the scavenger for •OH. Although previous experimental results indicated that lower pH increased $G(H_2O_2)$,[32] $G(H_2O_2)$ is stable in pH from 8 to 5. CO_2 radiolysis produces CO and O_2, and both of them can serve as a scavenger for e^-_{aq}. Previous study[38] has shown that the G-value of O_2 produced by CO_2 radiolysis is 2.24 for 1.5 MeV protons at 27°C and 0.4 atm pressure. Therefore, increased $G(H_2O_2)$ of water containing CO_2 might originate from O_2 production. In addition, CO_2 can directly react with e^-_{aq} (rate constant = 0.77×10^{10} $M^{-1}s^{-1}$),[39] and the reaction product, $CO_2{}^-$, can interact with various radicals and molecules, such as •OH and N_2O.[40] The detailed reason needs further investigation, and it would benefit

Monte Carlo radiochemical studies since CO_2 has been ignored in Monte Carlo codes.

We have discussed why, for real hypoxic water and normoxic water, the $G(H_2O_2)$ of three-spilled carbon ion UHDR is the same as that of three-spilled UHDR, unlike the experimental results with the electron beam. However, for hypoxic water, the $G(H_2O_2)$ of three-spilled carbon ion UHDR is higher than that of one-spilled UHDR. The only difference between hypoxic water and real hypoxic water is 5% CO_2, so this phenomenon is caused by CO_2. The possible reason is similar to CO_2 increasing the $G(H_2O_2)$: the first spill of carbon ion FLASH beam causes the CO_2 radiolysis to produce more O_2 in the environment, thereby increasing the $G(H_2O_2)$ of the subsequent spills, or the product of the reaction of CO_2 with e^-_{aq}, CO_2^-, participates in the subsequent reactions.

5 | LIMITATIONS

In our experiments, we bubbled water with pure N_2O gas for at least 40 min at room temperature. The main problem is we do not know the accurate N_2O concentration in each sample. First, we have to assume that N_2O molecules diffuse homogeneously in the bottle of water after 40 min of bubbling. Second, for real hypoxic water after bubbling N_2O, we brought the bottle of water back into the hypoxic chamber to fill water samples in 200 µL Eppendorf tubes. Therefore, the temperature change from room temperature to 37°C in the hypoxic chamber may have an impact on the N_2O concentration in the water. Besides, bubbling N_2O gas might influence the concentrations of other gases in the water. However, the conclusion is not affected since the comparison between UHDR, and conventional irradiation was done by the samples with the same solute gases. In future research, it would be beneficial to accurately measure the N_2O concentration in each sample and to test a range of different N_2O concentrations in the experiment. When considering these results in relation to the FLASH effect, one must be aware that these investigations were carried out in pure water, not in a biological system. Due to the existence of various antioxidant enzymes in living cells, radiochemistry might not be the same. What we found in water radiolysis needs to be investigated further with biologically relevant samples, such as an in-vitro study, to determine its significance in FLASH radiotherapy.

6 | CONCLUSION

For water samples with different O_2 and CO_2 concentrations (real hypoxic, normoxic, and hypoxic water), compared with conventional irradiation, UHDR always reduces the H_2O_2 production, regardless of whether high-LET or low-LET beams are used. O_2 and CO_2 can both increase H_2O_2 production, and CO_2 has a much higher solubility than O_2, which should not be ignored. The scavengers of e^-_{aq}, such as N_2O and $NaNO_3$, can narrow the difference in H_2O_2 production between UHDR and conventional irradiation, making it statistically insignificant, which suggests that UHDR produces less H_2O_2 because e^-_{aq} scavenging •OH, the precursor of H_2O_2, benefits more from the instantaneous radical concentration increase than the •OH self-reaction. The long-lived radical theory from previous Monte Carlo simulation studies that suggested that UHDR should produce more H_2O_2 cannot explain the results of the carbon ion UHDR experiment, indicating that this hypothesis cannot be the reason for the difference in H_2O_2 production between UHDR and conventional irradiation.

AUTHOR CONTRIBUTIONS

Conceptualization: Tengda Zhang. *Experimental methodology*: Tengda Zhang, Joao Seco and Kilian-Simon Baumann. *Investigation and methodology*: Tengda Zhang, Christina Stengl, Larissa Derksen, Kilian-Simon Baumann, Gerald Major, Kristaps Palskis, David Weishaar, Ulrike Theiß and Konstantinos Koritsidis. *Software*: Tengda Zhang, Christina Stengl, Larissa Derksen, Kilian-Simon Baumann, Kristaps Palskis and Konstantinos Koritsidis. *Formal analysis*: Tengda Zhang, Larissa Derksen, Kristaps Palskis and Konstantinos Koritsidis. *Data curation*: Tengda Zhang, Christina Stengl, Larissa Derksen, Kilian-Simon Baumann, Gerald Major, Ulrike Theiß, Kristaps Palskis and Konstantinos Koritsidis. *Visualization*: Tengda Zhang and Larissa Derksen. *Consultation*: Joao Seco, Kilian-Simon Baumann, Jürgen Hesser, Klemens Zink, Sebastian Adeberg, Jing Jin and Ulrike Theiß. *Supervision*: Joao Seco, Kilian-Simon Baumann, Jürgen Hesser, Klemens Zink, Sebastian Adeberg and Jing Jin. *Writing—original draft preparation*: Tengda Zhang. *Writing—review and editing*: Tengda Zhang, Christina Stengl, Larissa Derksen, Klemens Zink, Sebastian Adeberg, Gerald Major, Maria Francesca Spadea, Jing Jin, Jürgen Hesser, Kilian-Simon Baumann and Joao Seco. *Funding acquisition*: Joao Seco, Kilian-Simon Baumann, Klemens Zink and Sebastian Adeberg. All authors have read and agreed to the published version of the manuscript.

ACKNOWLEDGMENTS

The authors thank the MIT accelerator team for the beam settings, and the Preclinical Trial Unit at the DKFZ for their assistance with the x-ray irradiation. The project was partially supported by the Federal Ministry of Education and Research within the scope of the grant 'Biological and physical optimization of particle beams: radiation protection for the patient' (PARTITUR, grant number 02NUK076A). This study was partially funded by the

Hessen State Ministry of Higher Education, Research, and the Arts (HMWK) via the LOEWE Research Cluster "ADMIT", grant LOEWE/2/16/519/03/09.001(0001)/101. The experiments at MIT were supported by the Hessian state government. Larissa Derksen was supported by the Federal Ministry of Education and Research within the scope of the grant Physikalische Modellierung f¨ur die individualisierte Partikel-Strahlentherapie und Magnetresonanztomographie' (MiPS, Grant Number 13FH726IX6). Deutsche Krebshilfe (DKH) Grant with fördernummern 70115332, 70115445, and entitled "Dosisleistungsabhangige Ande¬rung des Sauerstoffpartlaldrucks wahrend FLASH-Bestrahlung und deren Einfluss auf die strahlenbi¬ologische Wirkung in Zebrafisch Embryonen".

Open access funding enabled and organized by Projekt DEAL.

CONFLICT OF INTEREST STATEMENT

The authors declare no conflicts of interest.

REFERENCES

1. Favaudon V, Caplier L, Monceau V, et al. Ultrahigh dose-rate FLASH irradiation increases the differential response between normal and tumor tissue in mice. *Sci Transl Med*. 2014;6(245):245ra93-245ra93.
2. Rohrer Bley C, Wolf F, Goncalves Jorge P, et al. Dose- and volume-limiting late toxicity of FLASH radiotherapy in cats with squamous cell carcinoma of the nasal planum and in mini pigs. *Clin Cancer Res*. 2022;28(17):3814-3823.
3. Vozenin MC, De Fornel P, Petersson K, et al. The advantage of FLASH radiotherapy confirmed in mini-pig and cat-cancer patients. *Clin Cancer Res*. 2019;25(1):35-42.
4. Le Caër S. Water radiolysis: influence of oxide surfaces on H2 production under ionizing radiation. *Water*. 2011;3(1):235-253.
5. Weiss H. An equation for predicting the surviving fraction of cells irradiated with single pulses delivered at ultra-high dose rates. *Radiat Res*. 1972;50(2):441-452.
6. Weiss H, Epp E, Heslin J, Ling C, Santomasso A. Oxygen depletion in cells irradiated at ultra-high dose-rates and at conventional dose-rates. *Int J Radiat Biol Relat Stud Phys Chem Med*. 1974;26(1):17-29.
7. Dahm-Daphi J, Sass C, Alberti W. Comparison of biological effects of DNA damage induced by ionizing radiation and hydrogen peroxide in CHO cells. *Int J Radiat Biol*. 2000;76(1):67-75.
8. Gülden M, Jess A, Kammann J, Maser E, Seibert H. Cytotoxic potency of H2O2 in cell cultures: impact of cell concentration and exposure time. *Free Radic Biol Med*. 2010;49(8):1298-1305.
9. Park WH. Hydrogen peroxide inhibits the growth of lung cancer cells via the induction of cell death and G1-phase arrest. *Oncol Rep*. 2018;40(3):1787-1794.
10. Ogawa Y. Paradigm shift in radiation biology/radiation oncology—exploitation of the "H2O2 effect" for radiotherapy using low-LET (linear energy transfer) radiation such as x-rays and high-energy electrons. *Cancers*. 2016;8(3):28.
11. Montay-Gruel P, Acharya MM, Petersson K, et al. Long-term neurocognitive benefits of FLASH radiotherapy driven by reduced reactive oxygen species. *Proc Natl Acad Sci*. 2019;116(22):10943-10951.
12. D-Kondo JN, Garcia-Garcia OR, LaVerne JA, et al. An integrated Monte Carlo track-structure simulation framework for modeling inter and intra-track effects on homogenous chemistry. *Phys Med Biol*. 2023;68(12):125008.
13. Kacem H, Psoroulas S, Boivin G, et al. Comparing radiolytic production of H(2)O(2) and development of zebrafish embryos after ultra high dose rate exposure with electron and transmission proton beams. *Radiother Oncol*. 2022;175:197-202.
14. Thomas W, Sunnerberg J, Reed M, et al. Proton and electron ultrahigh-dose-rate isodose irradiations produce differences in reactive oxygen species yields. *Int J Radiat Oncol Biol Phys*. 2024;118(1):262-267.
15. Wardman P. Radiotherapy using high-intensity pulsed radiation beams (FLASH): a radiation-chemical perspective. *Radiat Res*. 2020;194(6):607-617.
16. Sunnerberg JP, Zhang R, Gladstone DJ, Swartz HM, Gui J, Pogue BW. Mean dose rate in ultra-high dose rate electron irradiation is a significant predictor for O2 consumption and H2O2 yield. *Phys Med Biol*. 2023;68(16):165014.
17. Derksen L, Flatten V, Engenhart-Cabillic R, Zink K, Baumann K-S. A method to implement inter-track interactions in Monte Carlo simulations with TOPAS-nBio and their influence on simulated radical yields following water radiolysis. *Phys Med Biol*. 2023;68:135017.
18. Abolfath R, Grosshans D, Mohan R. Oxygen depletion in FLASH ultra-high-dose-rate radiotherapy: a molecular dynamics simulation. *Med Phys*. 2020;47(12):6551-6561.
19. Wardman P. Mechanisms of the 'FLASH'effect: radiation chemistry should not be ignored in developing models. *Radiother Oncol*. 2023;184:109673.
20. Lai Y, Jia X, Chi Y. Modeling the effect of oxygen on the chemical stage of water radiolysis using GPU-based microscopic Monte Carlo simulations, with an application in FLASH radiotherapy. *Phys Med Biol*. 2021;66(2):025004.
21. Hiroki A, Pimblott SM, LaVerne JA. Hydrogen peroxide production in the radiolysis of water with high radical scavenger concentrations. *J Phys Chem A*. 2002;106(40):9352-9358.
22. Boscolo D, Kramer M, Durante M, Fuss MC, Scifoni E. TRAX-CHEM: a pre-chemical and chemical stage extension of the particle track structure code TRAX in water targets. *Chem Phys Lett*. 2018;698:11-18.
23. Boyd A, Carver M, Dixon R. Computed and experimental product concentrations in the radiolysis of water. *Radiat Phys Chem*. 1980;15(2-3):177-185.
24. Plante I. A review of simulation codes and approaches for radiation chemistry. *Phys Med Biol*. 2021;66(3):03TR02.
25. Baikalov A, Abolfath R, Schüler E, Mohan R, Wilkens JJ, Bartzsch S. Intertrack interaction at ultra-high dose rates and its role in the FLASH effect. *Front Phys*. 2023;11:1215422.
26. Renault JP, Pommeret S. Seeing the solvated electron in action: first-principles molecular dynamics of NO3− and N2O reduction. *Radiat Phys Chem*. 2022;190:109810.
27. Frongillo Y, Goulet T, Fraser MJ, Cobut V, Patau JP, Jay-Gerin J-P. Monte Carlo simulation of fast electron and proton tracks in liquid water—II. nonhomogeneous chemistry. *Radiat Phys Chem*. 1998;51(3):245-254.
28. Town CD. Radiobiology. Effect of high dose rates on survival of mammalian cells. *Nature*. 1967;215(5103):847-848.
29. Epp ER, Weiss H, Santomasso A. The oxygen effect in bacterial cells irradiated with high-intensity pulsed electrons. *Radiat Res*. 1968;34(2):320-325.
30. Berry RJ, Hall EJ, Forster DW, Storr TH, Goodman MJ. Survival of mammalian cells exposed to x rays at ultra-high dose-rates. *Brit J Radiol*. 1969;42(494):102-107.
31. Limoli CL, Vozenin M-C. Reinventing radiobiology in the light of FLASH radiotherapy. *Annu Rev Cancer Biol*. 2023;7:1-21.
32. Sehested K, Rasmussen OL, Fricke H. Rate constants of OH with HO2, O2-, and H2O2+ from hydrogen peroxide formation in pulse-irradiated oxygenated water. *J Phys Chem*. 1968;72(2):626-631.

33. Wang H, Vassiliev ON. Radial dose distributions from carbon ions of therapeutic energies calculated with Geant4-DNA. *Phys Med Biol*. 2017;62(10):N219-N227.
34. Tian Z, Jiang SB, Jia X. Accelerated Monte Carlo simulation on the chemical stage in water radiolysis using GPU. *Phys Med Biol*. 2017;62(8):3081-3096.
35. Pastina B, LaVerne JA. Effect of molecular hydrogen on hydrogen peroxide in water radiolysis. *J Phys Chem A*. 2001;105(40):9316-9322.
36. Zakaria AM, Colangelo NW, Meesungnoen J, Azzam EI, Plourde M-É, Jay-Gerin J-P. Ultra-high dose-rate, pulsed (FLASH) radiotherapy with carbon ions: generation of early, transient, highly oxygenated conditions in the tumor environment. *Radiat Res*. 2020;194(6):587-593.
37. Burkholder J, Sander S, Abbatt J, et al. Chemical kinetics and photochemical data for use in atmospheric studies; evaluation number 19. 2020. https://jpldataeval.jpl.nasa.gov
38. Kummler R, Leffert C, Im K, Piccirelli R, Kevan L, Willis C. A numerical model of carbon dioxide radiolysis. *J Phys Chem*. 1977;81(25):2451-2463.
39. Buxton GV, Greenstock CL, Helman WP, Ross AB. Critical review of rate constants for reactions of hydrated electrons, hydrogen atoms and hydroxyl radicals (· OH/· O–) in aqueous solution. *J Phys Chem Ref Data*. 1988;17(2):513-886.
40. Neta P, Huie RE, Ross AB. Rate constants for reactions of inorganic radicals in aqueous solution. *J Phys Chem Ref Data*. 1988;17(3):1027-1284.

How to cite this article: Zhang T, Stengl C, Derksen L, et al. Analysis of hydrogen peroxide production in pure water: Ultrahigh versus conventional dose-rate irradiation and mechanistic insights. *Med Phys*. 2024;1-14. https://doi.org/10.1002/mp.17335